DOI: 10.1002/ejic.200900359

Thermally Stable Nanocrystalline Mesoporous Gallium Oxide Phases

Chinmay A. Deshmane,[a] Jacek B. Jasinski,[b] and Moises A. Carreon*[a]

Keywords: Mesoporous materials / Gallium oxides / Nanocrystals / Thermal stability / Heterogeneous catalysis

Semicrystalline and fully crystalline mesoporous gallium oxide phases were synthesized in the presence of ionic and non-ionic structure directing agents via Evaporation-Induced Self-Assembly (EISA) and Self-Assembly Hydrothermal-Assisted (SAHA) methods respectively. EISA led to partially crystalline mesoporous gallium oxide phases displaying unimodal pore size distribution in the range of ca. 2–5 nm and surface areas as high as 300 m^2/g. SAHA led to nanocrystalline mesoporous uniform micron-sized gallium oxide spheres (ca. 0.3–6.5 μm) with narrow size distribution displaying cubic spinel type structure. These mesophases displayed surface areas as high as ca. 221 m^2/g and unimodal pore size distribution in the 5–15 nm range. Textural properties such as surface areas and pore sizes were effectively fine-tuned by the nature and relative concentration of the structure directing agents. Due to their high surface areas, tunability of pore sizes and the nature of the wall structure, these gallium oxide mesophases could find potential applications as heterogeneous catalysts.

Introduction

Gallium oxides and gallium-based oxides are of great interest in the field of heterogeneous catalysis. Gallium oxide is a well known strong acid catalyst.[1] Ga_2O_3-based catalysts are active in the dehydrogenation of light alkanes[2] and in the selective catalytic reduction of NO_x by hydrocarbons in the presence of oxygen.[3] Supported gallium oxides are preferred over zeolites in the de-NO_x reaction because of their acidity.[4] These catalysts are also effective in the aromatization of ethane in the presence of CO_2.[2] Different polymorphs of gallium oxide have been employed for the dehydrogenation of alkanes to alkenes.[5,6] Recently, gallium oxide has been studied as catalyst in the epoxidation of cyclooctene in the presence of hydrogen peroxide.[7]

Gallium oxide has been synthesized using diverse techniques, such as thermal decomposition,[8] homogeneous precipitation using ammonia,[1,9,10] and surface layer adsorption.[11] However, these methods offer poor control over structural, morphological and compositional properties. It has been prepared in nanowire form by a number of techniques, including arc-discharge,[12,13] vapor-liquid-solid (VLS),[14,15] carbothermal reduction,[16,17] and thermal oxidation.[18,19] All these methods produced crystalline Ga_2O_3 nanowires with relatively low specific surface areas. Furthermore, these techniques are complex, time consuming and costly.

The surfactant-assisted self-assembly approach reported by researchers at Mobil Research and Development Corporation[20,21] represents an alternative and attractive method for the synthesis of novel transition metal oxide catalytic phases with desirable structural, compositional, and morphological properties.[22–24] Carreon and Guliants have reviewed the guiding principles for the synthesis of metal oxide mesostructures relevant to applications in catalysis.[24] Due to its unique and remarkable catalytic properties, gallium oxide is an attractive system for mesostructuring. Only few reports have been published on mesoporous gallium oxide synthesized employing surfactants as structure directing agents. Yada et al.[1,9] synthesized mesostructured gallium oxide, with hexagonal and layered structures by employing sodium dodecyl sulfate as the structure directing agent (SDA). Although the resultant mesophases displayed relatively high surface areas, they showed poor crystallinity and were thermally unstable at temperature above 300 °C.

Herein, we present the synthesis of thermally stable mesoporous gallium oxide employing, Evaporation-Induced Self-Assembly (EISA) and Self-Assembly Hydrothermal-Assisted (SAHA) approaches. These methods not only eliminate the need for high synthesis temperatures commonly required for solid-state reactions, but also offer the possibility to synthesize thermally stable mesoporous oxides with controlled morphological, textural and structural properties. EISA led to the formation of semi-crystalline gallium oxide mesophases displaying high surface area and unimodal pore sizes. SAHA led to the formation of fully crystalline micron-size gallium oxide mesoporous hollow spheres.

[a] Department of Chemical Engineering, University of Louisville, Louisville, KY 40292, USA
Fax: +1-502-8526355
E-mail: macarr15@louisville.edu
[b] Institute for Advanced Materials and Renewable Energy, University of Louisville,
Louisville, KY, USA

Supporting information for this article is available on the WWW under http://dx.doi.org/10.1002/ejic.200900359.

Results and Discussion

Current synthesis methods for the preparation of mesoporous gallium oxide offer limited control over structural, morphological and textural properties limiting its catalytic performance in heterogeneous catalysis. Self-assembly of inorganic precursors in the presence of liquid crystalline phases represent a promising route to overcome these limitations. First, we discuss the Evaporation-Induced Self-Assembly (EISA) and then the Self-Assembly Hydrothermal-Assisted (SAHA) approach.

EISA

EISA is a well-suited approach to prepare ordered mesophases with fine tuned structural and morphological properties.[25,26] In this study, cationic surfactant (CTAB) and non-ionic triblock copolymers (P123 and F127) were used as the structure directing agents to guide the mesostructure formation. The resulting as-synthesized mesophases were treated thermally to stabilize the inorganic framework and eliminate the SDA. At the synthesis pH of about 2, the dominant species in the solution are polycations[27,28] since the isoelectric point of gallium hydroxo species is about 9.[29] Therefore, the assembly process was likely controlled by electrostatic charge-matching between the inorganic ions in solution (I^+) charged surfactant headgroups (S^+) or non-ionic surfactants (S°) and inorganic counterions (NO^{3-}). Positively charged gallium hydroxo species assembled through hydrogen bonding mediation with CTAB or hydronium ion solvated neutral block copolymers. A similar mediated mechanism has been proposed for ordered mesoporous silica phases.[30,31]

Mesoporous oxides synthesized by employing F127 and P123 as SDA by EISA led to the formation of porous non-homogeneous in size spheres as seen in Figure 1. The average sphere size of the mesophase prepared with F127 as SDA was in the 0.05 to 0.5 μm range (Figure 1, A), while the average sphere size of the mesophases prepared by employing P123 as SDA were in 0.06 to 0.2 μm range (Figure 1, B). This Figure shows the porous nature of the spheres displaying average pore size of about 4–4.5 nm in agreement with pore size analysis. The samples prepared with CTAB as structure directing agent showed irregular morphologies.[32]

Table 1 summerizes general synthesis conditions and textural properties of the mesoporous gallium oxide phases obtained by EISA approach. Surface area as high as 298 m^2/g with unimodal average pore sizes in the range of about 2 to 4.6 nm were obtained. The nature of the structure directing agents helped to fine tune the pore size of the resulting mesophases. For instance, CTAB, F127, and P123 led to the formation of mesophases with average pore size of 2.0–2.8, 3.2–3.6, and ca. 4.2–4.6 nm, respectively. Due to its larger micellar size, amphiphilic block copolymers led to larger average pore sizes.

All the samples (E1–E6) displayed type-IV isotherms typical of mesoporous materials.[33,34] Figure 2 shows the N_2 adsorption–desorption isotherms and BJH pore size distributions from adsorption branch of the mesoporous gallium oxide phases synthesized by EISA. For example, the sample synthesized using CTAB as SDA (Figure 2, A), had a specific surface area of ca. 144 m^2/g with average unimodal pore diameter of ca. 2.8 nm. The sample synthesized using F127 as the SDA (Figure 2, B) showed a specific surface area of ca. 173 m^2/g and average pore diameter of ca. 3.6 nm. The sample synthesized using P123 as SDA (Figure 2, C) displayed a specific surface area of ca. 152 m^2/g and average pore diameter of ca. 4.2 nm. The isotherms for samples E2, E4 and E6 are shown elsewhere.[32]

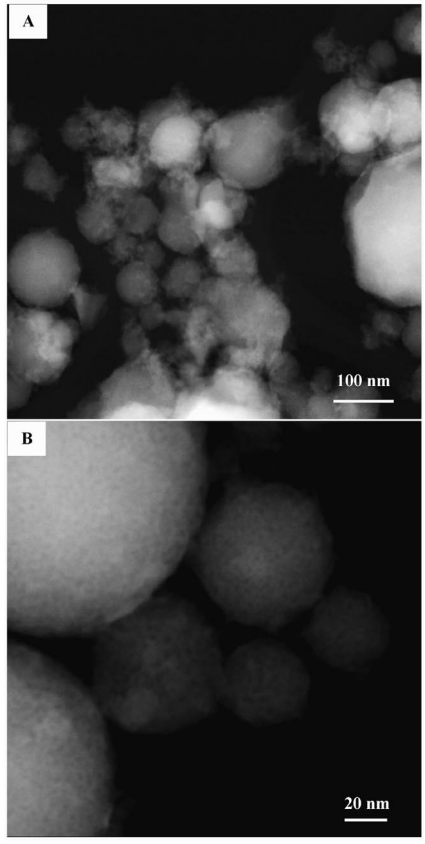

Figure 1. TEM images of mesoporous gallium oxide synthesized by EISA employing A) F127 and B) P123 as SDA.

Table 1. Synthesis conditions and textural properties of mesoporous gallium oxide phases synthesized by EISA.

Sample	Surfactant / amount [g]	Processing conditions T [°C] / RH (%)	Surface area [m^2/g]	Pore diameter [nm]	Pore volume [cm^3/g]
E1	CTAB / 0.3	30 / 65	144	2.8	0.11
E2	CTAB / 0.5	30 / 65	298	2.0	0.12
E3	F127 / 0.5	35 / 85	173	3.6	0.16
E4	F127 / 1.0	35 / 85	187	3.2	0.15
E5	P123 / 0.3	30 / 65	152	4.2	0.16
E6	P123 / 0.8	30 / 65	173	4.6	0.20

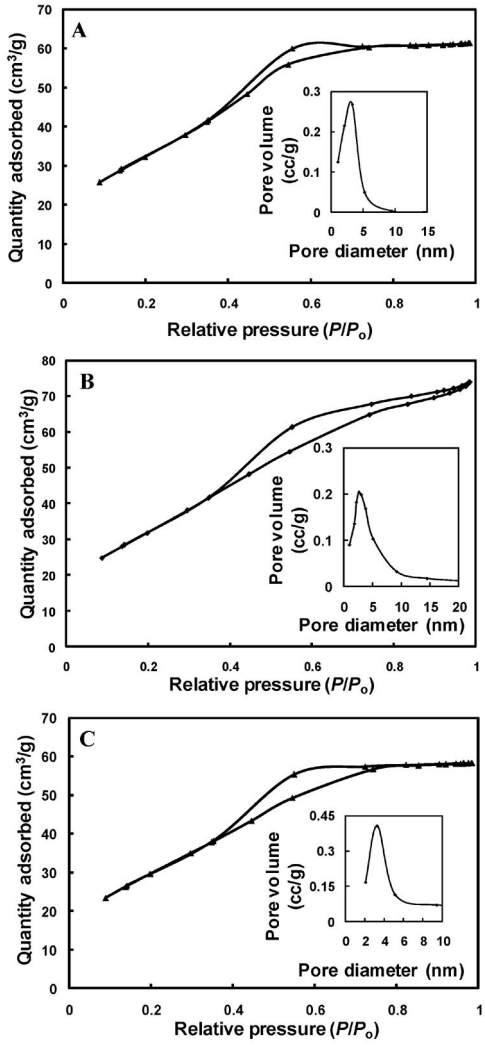

Figure 2. N_2 adsorption–desorption isotherms and BJH pore size distribution from adsorption branch of mesoporous gallium oxide phases synthesized by EISA employing A) CTAB (E1), B) F127 (E3), and C) P123 (E5) as SDA.

The mesostructure formation was confirmed by low-angle XRD.[32] These mesostructures showed a single broad peak at a $d_{spacing}$ of 40.7, 42.9, and 42.5 Å for the samples prepared with CTAB, F127, and P123 as SDA respectively, suggesting the formation of a wormhole mesostructure. High-angle X-ray diffraction patterns for these three samples displayed two broad peaks tentatively assigned to the (311) and (440) planes of cubic spinel confirming the semi-crystalline nature of the mesoporous walls as seen in Figure 3.

Selected area electron diffraction (SAED) of samples synthesized by EISA employing P123 as SDA yields a diffuse ring pattern indicating fine nanocrystalline or nearly amorphous structure. Two broad rings are observed (Figure 4, A) and their average $d_{spacing}$ of about 0.25 and 0.15 nm correlate well with the $d_{spacing}$ of (311) and (400) planes in a spinel-type cubic Ga_2O_3.[10,35] The intensity line

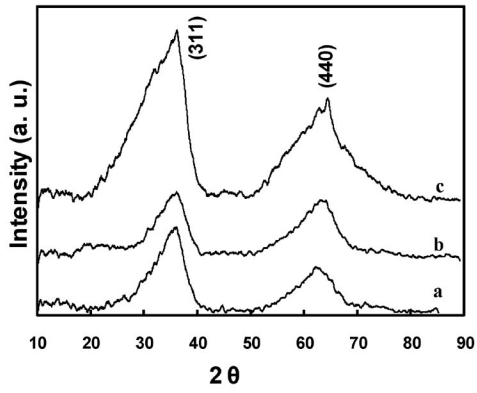

Figure 3. High-angle XRD patterns of mesoporous gallium oxide phases synthesized by EISA employing a) CTAB, b) F127, and c) P123 as SDA. X-ray radiation $Cu_{K\alpha}$ (λ = 1.54 Å).

profile measured across the SAED pattern (Figure 4, B) resembles high-angle XRD patterns obtained from EISA-synthesized samples (Figure 3, B).

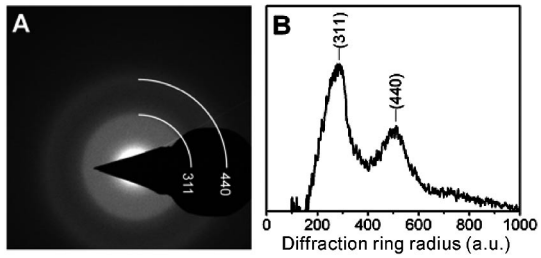

Figure 4. A) SAED pattern and B) intensity profile measured for mesoporous gallium oxide synthesized by EISA employing P123 as SDA.

SAHA

For many structure-sensitive applications, such as in heterogeneous catalysis, it is highly desirable to have a well-defined crystalline phase. In this respect, SAHA approach is an alternative self-assembly method to prepare nanocrystalline mesoporous gallium oxide phases. Nanocrystalline micron-sized mesoporous gallium oxide spheres with narrow particle size distribution prepared by using different structure directing agents are shown in Figure 5. The average size of the spheres obtained at hydrothermal temperature of 180 °C varied from about 2–3 μm. These nanocrystalline mesophases showed relatively high specific surface areas and unimodal pore size distribution as shown in Table 2. In general, it was observed that as the hydrothermal treatment temperature increased the specific surface area decreased, the average pore diameter increased, and the average sphere size increased.

The nitrogen adsorption–desorption isotherms and BJH pore size distributions from the adsorption branch of these nanocrystalline mesoporous gallium oxide phases synthesized employing CTAB (S1), F127 (S3), and P123 (S6), are shown in Figure 6. The shape of the isotherms and the hys-

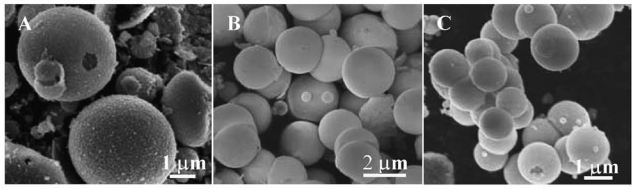

Figure 5. SEM images of mesoporous gallium oxide phases synthesized by SAHA at 180 °C employing A) CTAB (3 μm), B) F127 (2.2 μm), and C) P123 (2.0 μm) as SDA.

Table 2. General synthesis conditions and textural properties and average sphere size of mesoporous nanocrystalline gallium oxide phases synthesis by SAHA.

Sample	Surfactant / amount [g]	Hydrothermal temperature T [°C]	Surface area [m^2/g]	Pore diameter [nm][a]	Pore volume [cm^3/g]
S1	CTAB / 0.5	180	139	4.9 [3.0]	0.21
S2	CTAB / 1.0	200	107	5.6 [4.5]	0.16
S3	F127 / 0.5	180	152	4.3 [2.2]	0.20
S4	F127 / 1.0	200	122	7.6 [2.5]	0.30
S5	P123 / 0.3	180	123	11.5 [2.0]	0.26
S6	P123 / 0.9	200	70	12.2 [6.5]	0.26

[a] The numbers in the square brackets represent the average sphere size of the samples synthesized by SAHA.

teresis loops for all the samples indicated the mesoporous nature of these materials.[33,34] The sample synthesized with CTAB (Figure 6, A) showed a specific surface area of ca. 139 m^2/g with average unimodal pore diameter of ca. 5.0 nm. The mesophase synthesized using F127 (Figure 6, B) displayed a specific surface area of ca. 152 m^2/g and an average pore diameter of ca. 4.3 nm. The sample synthesized with P123 (Figure 6, C) showed a specific surface area of ca. 70 m^2/g with an average pore diameter of ca. 12.2 nm. The high surface area, unimodal pore size distribution, and nanocrystalline nature of these mesophases, are highly desirable properties for potential applications in heterogeneous catalysis. All mesophases were stable up to 450 °C.[32] At this temperature a decrease of surface area (ca. 10–40%) was observed. TGA showed that only ca. 1.6% and ca. 1.2% pyrolized template remained occluded in the pores of the mesoporous gallium oxide phases calcined at 350 and 450 °C, respectively.[32]

The high-angle X-ray diffraction patterns of a gallium oxide mesophases synthesized employing CTAB, F127 and P123 as SDA are shown in Figure 7. The high-angle XRD patterns, revealed strong reflections at $d_{spacing}$ = 4.7, 2.5, 2.02, 1.6, and 1.5 Å corresponding to the (111), (311), (400), (333), and (440) planes of cubic spinel type respectively (Figure 7). The high-angle XRD patterns observed for these mesophases are in agreement with previous reports.[10,35]

SAED pattern obtained for sample synthesized by SAHA employing F127 as SDA is shown in Figure 8 (A), whereas its intensity line profile is shown in Figure 8 (B). A spot-like form of the pattern and sharp, well-defined diffraction rings are the indications of a large-grain nanocrystalline material morphology, which is in agreement with TEM observations and XRD data. SAED ring diameter

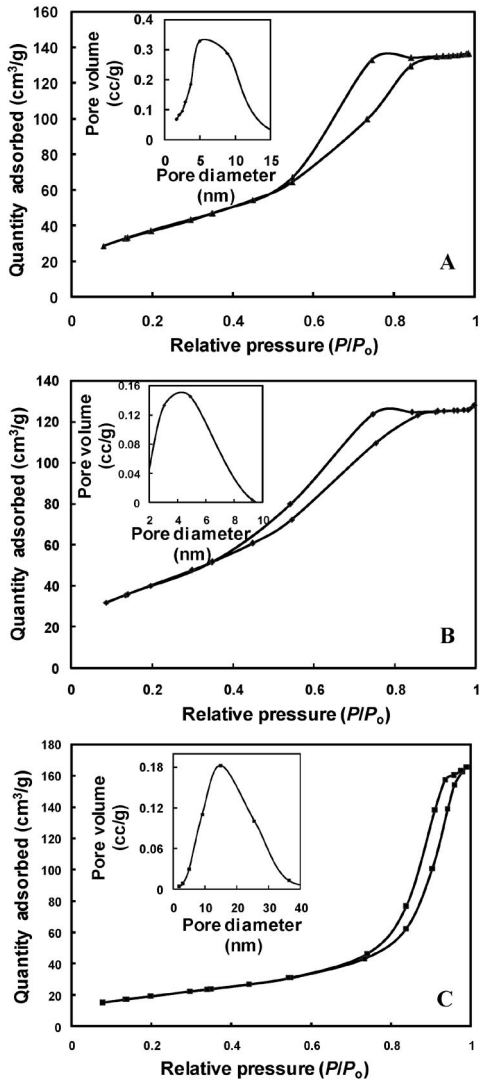

Figure 6. N_2 adsorption–desorption isotherms and BJH pore size distribution from adsorption branch of nanocrystalline gallium oxide phases synthesized by SAHA and employing A) CTAB, B) F127, and C) P123 as SDA.

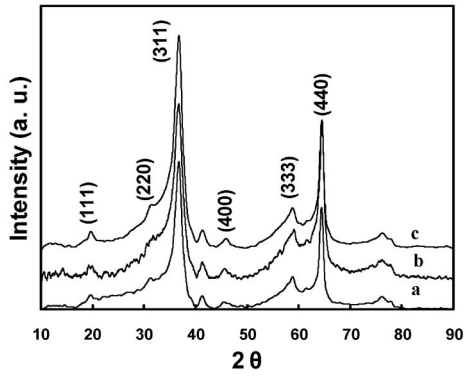

Figure 7. High-angle XRD patterns of mesoporous gallium oxide phases synthesized by SAHA employing a) CTAB, b) F127, and c) P123 as SDA. X-ray radiation $Cu_{K\alpha}$ (λ = 1.54 Å).

measurements, performed after using a standard gold specimen and calibrating the camera constant, provided the following $d_{spacing}$ values: 0.466, 0.285, 0.249, 0.222, 0.203, 0.192, 0.160, and 0.147 nm. All diffraction rings but the one corresponding to the $d_{spacing}$ of 0.222 nm could be unequivocally indexed within a spinel-type cubic structure. The cubic lattice parameter $a = 0.829 \pm 0.003$ nm, derived from the two most intense and sharp rings [e.g. (311) and (440)], agrees very well with the value reported previously for Ga_2O_3.[10,35]

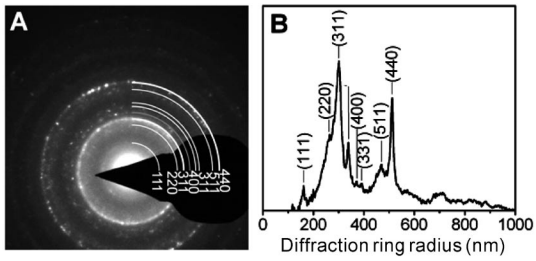

Figure 8. A) SAED pattern and B) intensity profile measured for mesoporous gallium oxide synthesized by SAHA.

HRTEM image of several nanocrystals present on the surface of the spheres (sample synthesized with F127 as SDA) is shown in Figure 9 (A). Lattice fringes are clearly visible in this image confirming the crystallinity of the material. The orientation of the nanocrystal on the left side of the image coincides with one of the main crystallographic directions resulting in the strong visibility of two perpendicular sets of lattice fringes. For clarity, the area marked by the square is magnified in Figure 9 (B). In addition, the bottom left quarter of the magnified image was enhanced by mask filtering of its Fourier transform (FT). Fringe spacing values of 0.25 and 0.29 nm were measured for these two sets of lattice fringes, as shown in the image. They coincide with the $d_{spacing}$ of {311} and {220} families of planes in previously mentioned spinel-type cubic Ga_2O_3. This is also in agreement with the FT produced from this HRTEM image (Figure 9, C). The FT can be consistently indexed when the (311) and (00$\bar{2}$) reflection are chosen for the base, which leads to the [$\bar{2}$33] zone axis pattern.

The samples synthesized by employing F127 as the SDA showed the highest surface areas as compared to CTAB or P123. We therefore present the effect of hydrothermal temperature as a function of sphere size on the samples synthesized using F127 as structure directing agent in Figure 10. At hydrothermal temperature of 150 °C, the average size of the spheres was ca. 1.8 μm (Figure 10A), the size increased to ca. 2.2 μm at 180 °C (Figure 10B) and to 4.5 μm (Figure 10, C) at 200 °C. Therefore, by adjusting the hydrothermal treatment temperature, micron-sized spheres of different sizes were obtained. A similar trend was observed for the samples synthesized employing CTAB and P123 as the structure directing agents.[32]

Smaller nanocrystalline mesoporous gallium oxide spheres were obtained when ethylene glycol was used as an organic additive as shown in Figure 11A. The addition of ethylene glycol resulted in the formation of uniform 0.3–

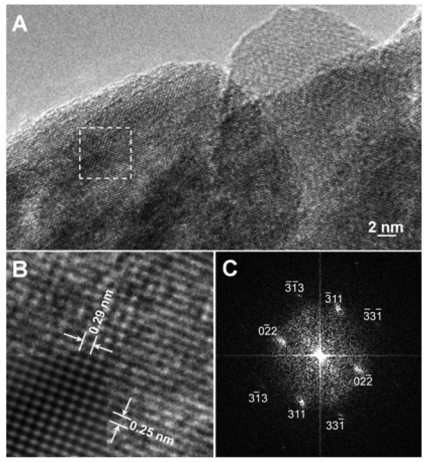

Figure 9. A) HRTEM image of nanocrystals on the surface of the mesoporous gallium oxide spheres synthesized by SAHA. B) Magnified image and C) FT of the area marked with dashed square in A.

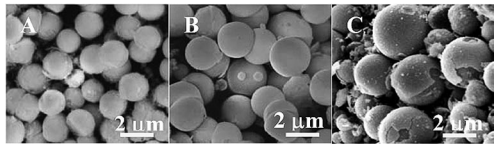

Figure 10. SEM images showing the effect of hydrothermal temperature on sphere size at A) 150 °C, B) 180 °C, and C) 200 °C employing F127 as SDA.

0.7 μm sized hollow spherical particles that are characterized by smooth surfaces. Ethylene glycol serves as a reagent that is able to mediate nucleation and growth, and thus improves the size uniformity of the resultant colloids.[36] Figure 11 (B) shows the TEM micrograph of this nanocrystalline gallium oxide mesophase prepared by employing hydrothermal temperature of 180 °C. These hollow spheres have a shell thickness of about 30 nm and the surface of the particles is covered with nanocrystals of size ca. 14 nm. High-angle XRD patterns indicated the formation of cubic spinel-type structure.[32]

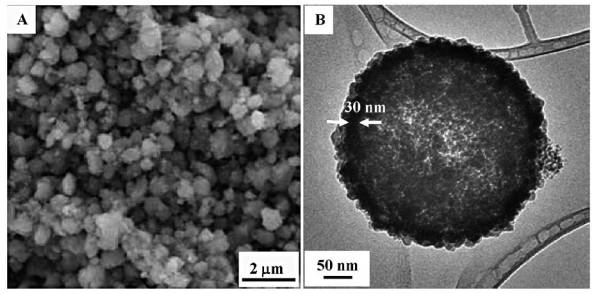

Figure 11. A) SEM and B) TEM images of mesoporous nanocrystalline gallium oxide phases obtained by SAHA and employing F127 as SDA and ethylene glycol as an organic additive.

Figure 12 shows the nitrogen adsorption–desorption isotherms and BJH pore size distribution from adsorption branch of mesoporous nanocrystalline gallium oxide phases

synthesized by SAHA and employing different concentrations of ethylene glycol and hydrothermal temperature of 180 °C. Type IV isotherms with H2 hysteresis loop confirmed the formation of the mesostructure. The sample prepared with 0.5 mL of ethylene glycol showed a specific surface area of ca. 175 m^2/g and an average unimodal pore diameter of ca. 7.3 nm (Figure 12, A). The sample synthesized using 2 mL of ethylene glycol showed a specific surface area of ca. 221 m^2/g with average unimodal pore diameter of ca. 5.2 nm (Figure 12, B). Therefore, the concentration of ethylene glycol allows one to fine tune the textural properties of the resultant mesophases.

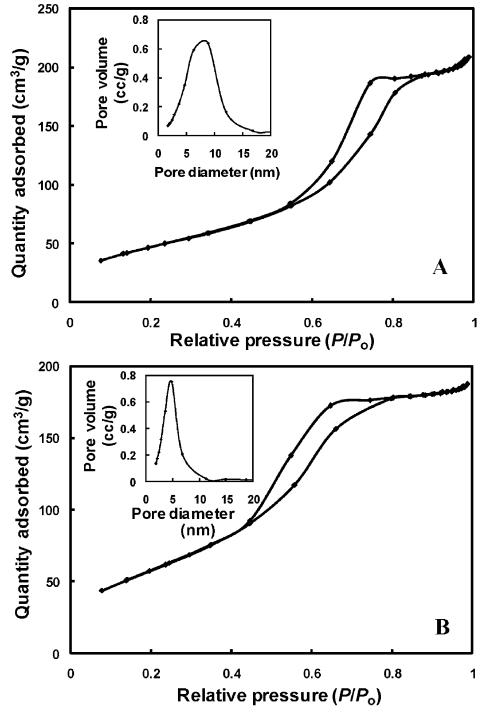

Figure 12. N_2 adsorption–desorption isotherms and BJH pore size distribution from adsorption branch of mesoporous gallium oxide synthesized by SAHA employing F127 as SDA and A) 0.5 mL of ethylene glycol and B) 2 mL of ethylene glycol as an organic additive.

The macroscopic morphology of mesoporous oxide phases is dictated by the local curvature energy present at the interface of the inorganic species and the amphiphilic surfactant species.[37] In particular a minimization of this local surface energy leads to sphere-like shapes.[38] Previous reports on mesoporous silica spheres[37–39] suggest that the use of CTAB and triblock copolymers under acidic conditions, and the control of synthesis stirring rates in the 200–400 rpm range, (prevailing conditions in our synthesis) favour the surface energy minimization promoting the formation of spheres shapes. Other factors such as condensation rate of inorganic species, concentration of SDA and co-surfactants have been also proposed as potential shape controlling factors in the formation of mesoporous silica spheres.[37]

Conclusions

Thermally stable mesoporous gallium oxide phases were successfully synthesized by employing EISA and SAHA approaches, using CTAB, P123 and F127 as the structure directing agents. EISA produced semi-crystalline mesoporous gallium oxide phases that displayed unimodal pore size distribution in the 2–15 nm range and relatively high specific surface areas up to ca. 300 m^2/g. SAHA led to the formation of uniform nanocrystalline mesoporous gallium oxide hollow spheres with narrow size distribution and displaying a cubic-spinel type structure. The average size of the spheres was successfully adjusted in the range of about 0.3–6.5 μm. These mesophases displayed surface areas as high as 221 m^2/g with unimodal pore diameter in the 5–15 nm range. These mesophases are particularly attractive for catalytic applications because of their high surface areas, tunability of pore sizes, and nature of the wall structure.

Experimental Section

Materials: Gallium(III) nitrate hydrate (99.99%, Strem Chemicals) was used as the inorganic precursor. Hexadecyltrimethylammonium bromide (CTAB, 99%, Sigma), Pluronic P123 (BASF) and F127 (BASF) were used as structure directing agents (SDA). Ethanol (ca. 99% Sigma) and 1-butanol (ca. 99% Sigma–Aldrich) were used as the organic solvents. Ethylene glycol (ca. 99% Sigma–Aldrich) was used as an organic additive.

Synthesis of Mesoporous Gallium Oxide by EISA: Mesoporous gallium oxide was prepared under mild synthesis conditions by reacting alcoholic solutions of gallium nitrate hydrate with SDA solutions. In a typical synthesis, the inorganic precursor was dissolved in the organic solvent (ethanol or 1-butanol). The solution was vigorously stirred at 40 °C (280 rpm) until the precursor was dissolved completely. A homogeneous alcoholic solution of the different structure directing agents (CTAB, F127 or P123) was prepared at 40 °C. The molar concentrations of the SDA were varied between 6.1×10^{-3}–350×10^{-3} (0.3 to 1 g). The SDA alcohol solution was then added dropwise to the precursor solution under continuous stirring for about 30 min. During the entire process the temperature was kept constant at 40 °C. The gel was then transferred to a petri dish and kept in the temperature-humidity chamber (Associated Environmental Systems) that was set at the desired conditions (typically T = 30 °C, RH = 85%). The gel was aged in the temperature-humidity chamber for 48 h, and then dried completely at 60 °C for 24 h. The surfactant was removed by calcination in air at 350 °C for 6 h to yield the mesoporous oxide phase. Typical synthesis compositions on molar basis were precursor:surfactant:solvent = 1:(6.1×10^{-3} to 350×10^{-3}):9.

Synthesis of Hollow Mesoporous Nanocrystalline Gallium Oxide Spheres by SAHA: The synthesis procedure is similar to that followed in EISA. An inorganic precursor-alcoholic solution was mixed with the SDA solution and was homogenized for 30 min at 40 °C (280 rpm). The homogeneous gel was then transferred to a 45 mL Teflon®-lined stainless steel autoclave (Parr Instrument Company) and heated under autogenous pressure in a static condition in conventional oven at 150 °C–200 °C for 20 h. The resultant white solids were separated from the solution by centrifugation (4000 rpm, 20 min), washed three times with deionized water and dried overnight at 60 °C. The fine powder was then calcined in air at 350 °C for 6 h yielding mesoporous hollow nanocrystalline gal-

lium oxide spheres. In some synthesis, ethylene glycol was used as an organic additive to reduce the size of the mesoporous oxide hollow spheres. Ethylene glycol was added dropwise to the homogeneous gel with constant stirring and then transferred to the Teflon®-lined stainless steel autoclaves and placed in the oven for hydrothermal treatment at different temperatures (180 °C, 200 °C) for 8 h (Figures 11 and 12). The concentration of ethylene glycol on molar basis varied in the 2–8.3 range. Typical synthesis compositions employed for SAHA were similar to those used for EISA.

Characterization: The morphology and crystal size of the mesophases were analyzed with a FE-SEM (FEI Nova 600) with an acceleration voltage of 6 kV. The XRD patterns were collected on Bruker D8 Discover diffractometer employing $Cu_{K\alpha}$ (λ = 1.54 Å) as the source. N_2 adsorption BET surface areas were determined in a Micromeritics Tristar-3000 porosimeter. Before the surface area measurements, the samples were degassed at 300 °C for 3 h. TEM and HRTEM images were collected on Technai F20 FEI TEM using a field emission gun, operating with an accelerating voltage of 200 kV.

Supporting Information (see also the footnote on the first page of this article): N_2 adsorption–desorption isotherms and BJH pore size distribution from adsorption branch of samples E2, E4 and E6, HRTEM image displaying the porous nature of mesoporous gallium oxide synthesized by EISA, SEM images showing the effect of hydrothermal temperature on the particle size of mesoporous gallium oxide phases synthesized by SAHA employing CTAB and P123 as SDA, N_2 adsorption–desorption isotherms and BJH pore size distribution from adsorption branch of samples S2, S4 and S5, low-angle XRD patterns of mesporous gallium oxide samples synthesized by EISA, high-angle XRD patterns of mesoporous gallium oxide phases prepared by SAHA employing F127 as SDA and ethylene glycol as an additive, N_2 adsorption–desorption isotherms and BJH pore size distribution from adsorption branch of samples synthesized by EISA and SAHA calcined at 450 °C, TGA profiles for the mesoporous gallium oxides calcined at 350 and 450 °C.

[1] M. Yada, M. Ohya, M. Machida, T. Kijima, *Langmuir* **2000**, *16*, 4752.
[2] K. Nakagawa, C. Kajita, Y. Idle, M. Okamura, S. Kato, H. Kasuya, N. Ikenaga, T. Suzuki, *Catal. Lett.* **2000**, *64*, 215.
[3] K. Shimizu, A. Satsuma, T. Hattori, *Appl. Catal. B* **1998**, *16*, 319.
[4] K. Bethke, M. Kung, B. Yang, M. Shah, D. Alt, C. Li, H. Kung, *Catal. Today* **1995**, *26*, 169.
[5] B. Zheng, W. Hua, Y. Yue, Z. Gao, *J. Catal.* **2005**, *232*, 143.
[6] K. Nakagawa, M. Okamura, N. Ikenaga, T. Suzuki, T. Kobayashi, *Chem. Commun.* **1998**, 1025.
[7] a) P. P. Pescarmona, K. P. F. Janssen, P. A. Jacobs, *Chem. Eur. J.* **2007**, *13*, 6562; b) P. P. Pescarmona, P. A. Jacobs, *Catal. Today* **2008**, *137*, 52.
[8] P. Michorczyk, J. Ogonowski, *Appl. Catal. A: General* **2003**, *251*, 425.
[9] M. Yada, H. Takenaka, M. Machida, T. Kijima, *J. Chem. Soc., Dalton Trans.* **1998**, 1547.
[10] a) C. O. Areán, A. L. Bellan, M. P. Mentruit, M. R. Delgado, G. T. Palomino, *Microporous Mesoporous Mater.* **2000**, *40*, 35; b) M. R. Delgado, C. O. Areán, *Mater. Lett.* **2003**, *57*, 2292.
[11] X. Sun, Y. Li, *Angew. Chem. Int. Ed.* **2004**, *43*, 3827.
[12] Y. C. Choi, W. S. Kim, Y. S. Park, S. M. Lee, D. J. Bae, Y. H. Lee, G. S. Park, W. B. Choi, N. S. Lee, J. M. Kim, *Adv. Mater.* **2000**, *12*, 746.
[13] W. Q. Han, P. Kohler-Redlich, F. Ernst, M. Ruhle, *Solid State Commun.* **2000**, *115*, 527.
[14] C. H. Liang, G. W. Meng, G. Z. Wang, Y. M. Wang, L. D. Zhang, *Appl. Phys. Lett.* **2001**, *78*, 3202.
[15] H. J. Chun, Y. S. Choi, S. Y. Bae, H. W. Seo, S. J. Hong, J. Park, H. Yang, *J. Phys. Chem. B* **2003**, *107*, 9042.
[16] X. C. Wu, W. H. Song, W. D. Huang, M. H. Pu, B. Zhao, Y. P. Sun, J. J. Du, *Chem. Phys. Lett.* **2000**, *328*, 5.
[17] G. Gundiah, A. Govindaraj, C. N. R. Rao, *Chem. Phys. Lett.* **2002**, *351*, 189.
[18] Z. R. Dai, Z. W. Pan, Z. L. Wang, *J. Phys. Chem. B* **2002**, *106*, 902.
[19] B. C. Kim, K. T. Sun, K. S. Park, K. J. Tm, T. Noh, M. Y. Sung, S. Kim, S. Nahm, Y. N. Choi, S. S. Park, *Appl. Phys. Lett.* **2002**, *80*, 479.
[20] C. T. Kresge, M. E. Leonowicz, W. J. Roth, J. C. Vartuli, J. S. Beck, *Nature* **1992**, *359*,710.
[21] J. S. Beck, J. C. Vartuli, W. J. Roth, M. E. Leonowicz, C. T. Kresge, K. D. Schmitt, C. T.-W. Chu, D. H. Olson, E. W. Sheppard, S. B. McCullen, J. B. Higgins, J. L. Schlenker, *J. Am. Chem. Soc.* **1992**, *114*, 10834.
[22] F. Schüth, *Chem. Mater.* **2001**, *13*, 3184.
[23] A. Taguchi, F. Schüth, *Microporous Mesoporous Mater.* **2005**, *77*, 1.
[24] M. A. Carreon, V. V. Guliants, *Eur. J. Inorg. Chem.* **2005**, *1*, 27.
[25] a) Y. Lu, H. Fan, A. Stump, T. L. Ward, T. Reiker, C. J. Brinker, *Nature* **1999**, *398*, 223; b) C. J. Brinker, Y. Lu, A. Sellinger, H. Fan, *Adv. Mater.* **2004**, *16*, 309.
[26] M. A. Carreon, V. V. Guliants, *Mesostructuring Metal Oxides through Evaporation Induced Self-Assembly: Fundamentals and Applications*, *Nanoporous Solids*, *Recent Advances and Prospects*, Elsevier, **2008**, *16*, p. 407.
[27] J. P. Jouliet, *Metal Oxide Chemistry and Synthesis: From Solution to Solid State*, Wiley, Chichester (U.K.), **2000**.
[28] C. J. Brinker, G. W. Scherer, *The Physics and Chemistry of Sol-Gel Processing*, Academic Press, Inc., **1990**.
[29] M. Kosmulski, *J. Colloid Interface Science* **2001**, *238*, 225.
[30] Q. Huo, D. I. Margolese, U. Ciesla, P. Feng, T. E. Gier, P. Sieger, R. Leon, P. M. Petroff, F. Schüth, G. D. Stucky, *Nature* **1994**, *368*, 317.
[31] a) G. Attard, J. C. Glyde, C. G. Goltner, *Nature* **1995**, *378*, 366; b) D. Zhao, J. Feng, Q. Huo, N. Melosh, G. H. Fredickson, B. F. Chmelka, G. D. Stucky, *Science* **1998**, *279*, 548.
[32] See supporting information.
[33] S. J. Greg, K. S. W. Sing, *Adsorption Surface Area and Porosit*, Academic Press, London, **1969**.
[34] M. A. Carreon, V. V. Guliants, L. Yuan, A. R. Hughett, A. Dozier, G. A. Seisenbaeva, V. G. Kessler, *Eur. J. Inorg. Chem.* **2006**, 4983; K. S. W. Sing, D. H. Everett, R. A. W. Haul, L. Moscou, R. A. Pierroti, J. Rouquerol, T. Siemieniewska, *Pure Appl. Chem.* **1995**, *57*, 603.
[35] R. Roy, V. G. Hill, E. F. Osborn, *J. Am. Chem. Soc.* **1952**, *74*, 719; S. W. Kim, S. Iwamoto, M. Inoue, *Ceramics Int.* **2009**, *35*, 1603.
[36] X. Jiang, T. Herricks, Y. Xia, *Adv. Mater.* **2003**, *15*, 15.
[37] D. Zhao, J. Sun, Q. Li, G. D. Stucky, *Chem. Mater.* **2000**, *12*, 275.
[38] H. Yang, G. Vovk, N. Coombs, I. Sokolov, G. A. Ozin, *J. Mater. Chem.* **1998**, *8*, 743.
[39] Q. Huo, J. Feng, F. Schuth, G. D. Stucky, *Chem. Mater.* **1997**, *9*, 14.

Received: April 20, 2009
Published Online: June 22, 2009

